Appl Phys A (2009) 95: 249–255
DOI 10.1007/s00339-008-5023-z

Applied Physics A
Materials Science & Processing

Application of MEH-PPV/SnO_2 bilayer as hybrid solar cell

Jose Antonio Ayllon · Monica Lira-Cantu

Received: 22 July 2008 / Accepted: 24 November 2008 / Published online: 18 December 2008

Abstract The applications of conducting organic polymers in combination with semiconductor oxides are promising candidates as active materials for air-stable hybrid electronic applications such as transistors, light emitting diodes or organic photovoltaics. In this work, we report our last results on the application of SnO_2 thin films in all solid-state hybrid solar cells. We also compare the results with other five solar cells developed in our laboratories applying MEH-PPV and semiconductor oxides like TiO_2, Nb_2O_5, ZnO, CeO_2 or CeO_2–TiO_2. In this work, SnO_2 thin films, obtained from sol–gel solutions, have been applied in HSC in a configuration ITO/$SnO_{2\ \text{thin film}}$/MEH-PPV/Ag. The effects of factors, such as UV light, polymer thickness, stabilization in the dark and performance under irradiation conditions, have been investigated. Open circuit voltage and short circuit current values were about −0.45 V and 0.17 mA/cm^2, with fill factors around 30%. Photoaction spectra show the activity of the semiconductor oxide below 340 nm and about 490 nm for the polymer. Lifetime behavior of the HSC showed an initial increase in current density reaching a maximum after about 1 h of irradiation. Blocking the UV-wavelength range by the application of a filter showed no significant difference in HSC properties with respect to the sample without UV filter. Comparison with other 5 semiconductor oxides revealed a direct relation between semiconductor oxide applied and V_{oc} from the solar cell.

PACS 72.40.+w · 78.20.-e · 78.66.-w

1 Introduction

The application of conducting organic polymers (COPs) in organic electronics is based on their ability to transport, emit or absorb light under specific conditions [1]. Thus, we can find COPs as part of the active layer of electronic devices such as transistors, LEDs or solar cells. In organic photovoltaic (OPVs) devices, COPs have been part of extensive research work, specially the combination of poly(3-hexylthiophene) (P3HT) and the C60 derivative ([6, 6]-phenyl-C61-butyric acid methyl ester) PCBM which has shown excellent PV properties with efficiencies beyond 5% [1–4]. The potential of OPVs resides in their low cost, not because of the low price of the materials applied, but due to the printing techniques applied for their fabrication [4]. Among the challenges to overcome for this technology are the improvement of solar cell efficiency and lifetime. Lifetime limitation resides in the degradation of the organic semiconductors due to the presence of oxygen or moisture from the atmosphere [5–7], thus encapsulation of these devices is a requirement [7]. Several attempts have been made in order to find new electron transport materials with better transport properties and higher stability towards oxygen. In this respect, semiconductor oxides emerged as an attracting alternative to replace PCBM in OPVs due to their appealing properties. Besides lower cost these oxides are wide bandgap materials able to accept electrons effectively. Furthermore, recent studies have shown the possibility of semiconductor oxides to work under ambient atmospheres when

J.A. Ayllon
Chemistry Department, Universitat Autonòma de Barcelona, Campus UAB, 08193 Bellaterra, Spain
e-mail: joseantonio.ayllon@uab.es
Fax: +34-93-5812920

M. Lira-Cantu (✉)
Centro de Investigaciò en Nanociencia i Nanotecnologia, CIN2 (CSIC-ICN), Campus UAB, Edifici ETSE 2nd Floor, 08193 Bellaterra, Barcelona, Spain
e-mail: monica.lira@cin2.es
Fax: +34-93-5813797

they are used in direct contact with conducting organic polymers in a electronic devices like solar cells [8–12] or more recently as air-stable OLEDs [13, 14].

We have recently analyzed different semiconductor oxides in HSC [8–12] and have documented a fine interaction between the semiconductor oxide and oxygen from the atmosphere. In an effort to broaden our knowledge on the interaction of these systems with air, we present here our results on the application of thin films of SnO_2 as electron acceptor in HSC. Analyses of the interaction of SnO_2 with conjugated polymers have been limited to a fundamental level [15–17], and other studies reported that the electron transfer from MEH-PPV to SnO_2 is energetically favorable and can be photoinduced [15]. Although, these processes are known to be slower than for TiO_2 (800 fs vs. less than 100 fs) the advantage for SnO_2 utilization is based on a more favorable position of its conduction band [15]. It is also known that the electron transfer rate from the polymer MEH-PPV and the SnO_2 is on the order of microseconds, yielding a possible candidate to construct HSCs [15]. Finally, the application of nanocrystalline thin films rather than isolated nanoparticles could be advantageous, as it increases the ability of the semiconductor to transport the charge to the electrode through the connected inorganic network [16]. We present in this work HSCs applying a device configuration of ITO/SnO_2 thin film/MEH-PPV/Ag. We analyzed the effect of polymer thickness and solar cell performance by I–V-curves, photophysical analyses, and especially lifetime studies. A brief discussion on the application of different semiconductor oxides already studied in our laboratories and their comparison with SnO_2 are also presented.

2 Experimental

2.1 Materials

MEH-PPV was synthesized as described in [8–12]. Indium tin oxide (ITO) substrates were purchased from Delta Technologies, Lt. (U.S.A.). The substrates dimensions were $25 \times 50 \times 1.1$ mm (coated on one surface, Rs = 10 ohms ± 5 ohms), and substrates were etched and prepared following a method described earlier [8–12]. Once etched, the substrates were washed with acetone and ethanol in an ultrasonic bath for 10 min, respectively. $SnCl_2$ $2H_2O$ and absolute ethanol were obtained from Panreac and used as received.

2.2 Preparation of SnO_2 thin films

Tin oxide sol precursor was prepared by dissolving 13.5 g of $SnCl_2$ $2H_2O$ (5.98×10^{-2} mol) in 100 ml of absolute ethanol and then refluxing during 2.5 h [18]. This solution was allowed to cool to room temperature, filtered and spin coated on top of ITO substrates. The as-prepared films were annealed at 450°C for two hours to completely oxidize the precursor and induce the crystallization of SnO_2.

2.3 Polymer photovoltaic preparation and characterization

The ITO/thin film semiconductor oxide substrate was first subjected to 100°C for 10 min to eliminate any possible absorbed water on the surface. The substrates were then cleaned with chloroform (via spin coating) and then a microfiltered MEH-PPV polymer solution (0.45 μm pore size) from chlorobenzene was spincoated at 1000 rpm or 1500 rpm on top of the ITO/semiconductor oxide substrates. The absorbance of the spincoated polymer films was controlled to be about 1.0 absorbance units unless otherwise specified. The active area of the devices was 3.2 ± 0.1 cm^2. Silver electrodes were thermally evaporated onto the polymer film at a pressure of $<10^{-5}$ mBar though a mask. The device was mounted using conductive silver epoxy glue for the electrical contacts. Final device configuration was ITO/$SnO_{2\text{thin film}}$/MEH-PPV/Ag. The positive terminal of the Keithley Sourcemeter was attached to the glass/ITO/oxide, and the negative terminal was attached to the metal electrode. This deliberate choice was made in order to distinguish the function of the transparent conducting oxide (TCO) and metal electrode as compared to traditional polymer photovoltaics where the TCO is the hole collector and the metal is the electron collector. Samples were then analyzed in the ambient atmosphere. As a measure of the decay we recorded the short circuit current (J_{sc}) as a function of time during illumination since the efficiency of the device and J_{sc} are linked as described earlier. Values of V_{oc} and J_{sc} were measured for the devices under ambient conditions and finally I–V-curves, action spectra and solar decay analyses were determined in that order for the devices. The wavelength dependence of the photovoltaic response was characterized using a set-up described earlier [8–12], and the photovoltaic response under AM1.5 simulated sunlight was performed using a SolarConstant 575 from Steuernagel Lichttechnik GmBH, Germany. The spectral distribution and quality of the solar simulator were monitored following the ASTM E927 standard recommendations using a spectrometer from AvaSpec 2048 from Avantes, and a Precision Pyranometer from Eppley Laboratories was used to monitor the total power that was set to 1000 W m^{-2} in all experiments. Polymer film thicknesses were analyzed by AFM.

3 Results and discussion

3.1 General characterization

Figure 1 shows the grazing incidence X-ray diffraction analysis of the SnO_2 thin film applied as electron acceptor for the hybrid solar cells reported in this work. For comparison purposes the diffractogram of the ITO, [91(In_2O_3) : 9(SnO_2)], substrate is also shown. These results confirm the correct formation of SnO_2 on the ITO substrate.

HSCs applying semiconductor oxides are stable in ambient atmospheres, and have been shown to stabilize and improve PV properties after storage in the dark under ambient atmosphere conditions [8–12]. Usually a few hours up to a couple of days is required for these solar cells to reach maximum performance. Storage in the dark in air can be made for several months, even years (up to 1.5 years in our laboratory) without significant degradation of photovoltaic properties. Thus, the HSCs analyzed in this work were stabilized in the dark for 1 h and 24 h under ambient atmosphere conditions before analyses. Figure 2 shows the I–V-curves carried out to HSCs applying two polymer thicknesses of 90 nm and 110 nm. In order to obtain different thicknesses, the same MEH-PPV polymer solution was coated on top of the SnO_2 layer at different spin coating speeds. The use of 1500 rpm resulted in a 90 nm polymer thicknesses, while the spin coating velocity fixed at 1000 rpm gave polymer films of 110 nm. Figures 2(a) and 2(b) show the I–V-curves obtained for devices with polymer thicknesses of 90 nm and 110 nm, respectively. We observed a small difference in shape between both graphs but, in general, both HSC showed almost the same V_{oc} and J_{sc} values around 0.3 V and 0.15–0.2 mA/cm^2; FFs were also in the

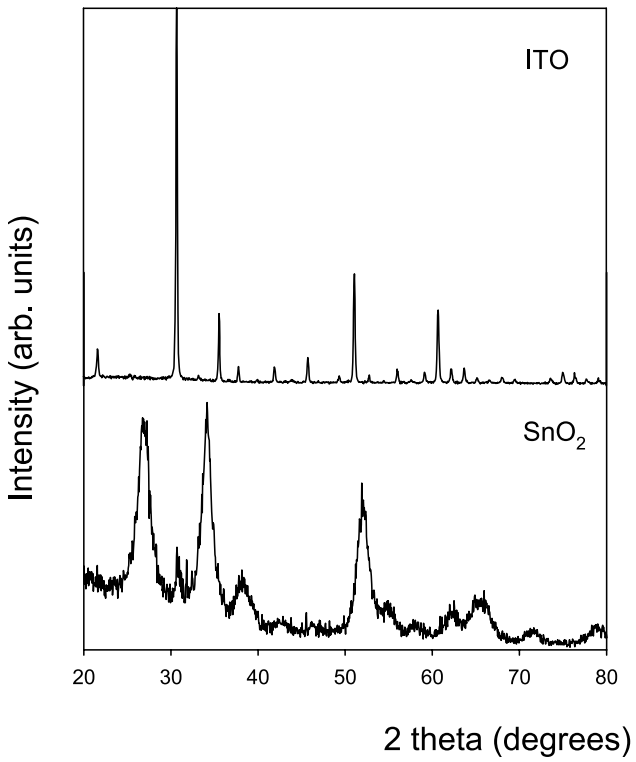

Fig. 1 Grazing incidence X-ray diffraction analysis of the SnO_2 thin film semiconductor oxide synthesized on ITO from sol–gel solution (diffraction angle 0.3 degrees). For comparison proposes the diffractogram of the ITO, [91(In_2O_3) : 9(SnO_2)], substrate is also shown

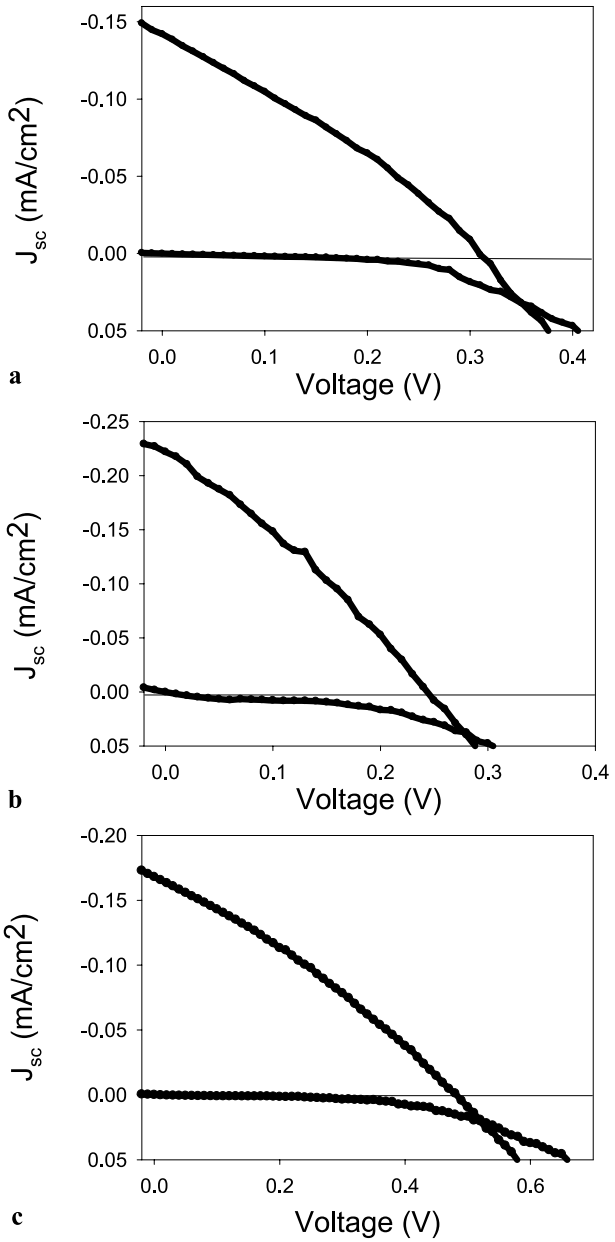

Fig. 2 I–V-curves for a hybrid solar cell (HSC) of the type ITO/$SnO_{2\ thin\ film}$/MEH-PPV/Ag with polymer thickness of (**a**) 110 nm, (**b**) 90 nm. Both cells were stabilized in the dark under ambient atmospheres for 1 h. (**c**) HSC stabilized for 24 h in the dark undercambient atmosphere, polymer thickness of 90 nm. HSCs measured in ambient atmosphere with AM1.5 spectral distribution and 1000 W/m^2. Active area is 3.2 ± 0.1 cm^2

same 26–28% range, as expected due to the similarity of the polymer thickness. These similar results show that a difference of 20 nm in polymer thickness between layers is not enough to produce meaningful effects on photovoltaic performance. Thus, a polymer thickness of 90 nm was chosen to study the HSC photovoltaic properties after the device was stabilized in the dark for 24 h. The HSC (90 nm polymer thickness), shown in Fig. 2(c), revealed that a 24 h period of stabilization in the dark improved V_{oc} values from 0.3 to 0.5 V, while J_{sc} was observed to be on the same range as before stabilization. The V_{oc} and J_{sc} values observed after stabilization were 0.5 V and 0.18 mA/cm^2, respectively, with a FF of 33%. As already reported for other HSC applying semiconductor oxides, we have attributed this behavior to the oxygen requirement of the semiconductor oxide [8–12]. It has been reported that a small oxygen loss from the semiconductor oxide structure can reduce and modify its photoconductivity properties [19], a condition that is present in our HSC during electrode evaporation which takes place under high vacuum conditions (1×10^{-6} mbar). In the case of SnO_2, however, this effect could also be influenced by its high sensitivity to different atmospheres [20]. Complete lifetime studies showed only 8 h of lifetime before device degradation.

3.2 Photophysical analyses

Photophysical analyses performed to the HSCs applying two polymer thicknesses are shown in Fig. 3(a) (labeled as I and II). For comparison purposes the UV–VIS spectra of the MEH-PPV polymer are also shown (Fig. 3(b)). The shape of the polymer spectra and that of the photoaction spectra of the HSC are similar, which suggests that the absorption of the polymer MEH-PPV is mainly responsible for the photocurrent generation in the cell. Moreover, the absorption band below 350 nm corresponds to the contribution of SnO_2.

A comparison of the absorption spectra of the MEH-PPV polymer (Fig. 3(b)) with the maxima of the photoaction spectra reveals a shift in the position of the wavelength band which corresponds to the MEH-PPV polymer. This shift has been observed in our HSCs independently of the thin film semiconductor oxide applied [10]. The presence of a blue shift in the action spectra has been observed before as an indication of the formation of a charge transfer complex (CTC) between the polymer and oxygen from the atmosphere as already reported [10]. Nevertheless, the photoaction spectra shown in Fig. 3(a) indicate a shift towards the UV–VIS (lower wavelengths) invalidating the possible formation of a CTC. The observed shift has been attributed to thin film interferences as also observed for other HSC applying other semiconductor oxides [8–12].

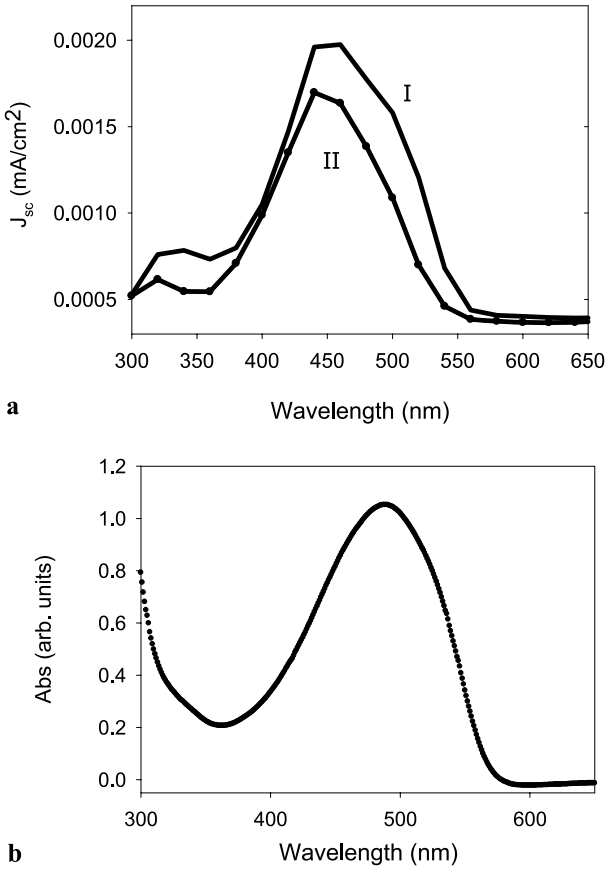

Fig. 3 Photophysical analyses of a hybrid solar cell of the type ITO/$SnO_{2\ thin\ film}$/MEH-PPV/Ag with two different polymer thicknesses (**aI**) 110 nm and (**aII**) 90 nm. For comparison purposes we show the UV–VIS absorbance spectra of the MEH-PPV (**b**). Active area is 3.2 ± 0.1 cm^2

3.3 Effect of UV-light

A well-known property of semiconductor oxides, like SnO_2, is their ability to absorb in the UV-wavelength range. The major advantage observed for SnO_2 is its electron affinity when compared with one of the best oxides, TiO_2 (CB edge TiO_2 : −4.2 eV vs. vacuum, and SnO_2 : −4.77 eV vs. vacuum) [21, 22]. Thus, we seek to understand if the degradation of the polymer observed when semiconductor oxides are applied in HSC as reported earlier [18, 22] can be reduced by the application of SnO_2 thin films, also to analyze its effect on overall solar cell performance. With this in mind, we carried out I–V-curve analyses of the HSC applying SnO_2, under conditions of light and under ambient atmosphere. By blocking the UV-light (applying a UV-filter) we were able to analyze the effect of the SnO_2 on the performance of the HSC.

A decrease in current density is expected during the application of the filter since a part of the UV-wavelength range at which the semiconductor is excited accounts for overall solar cell photocurrent. Nevertheless, unimportant

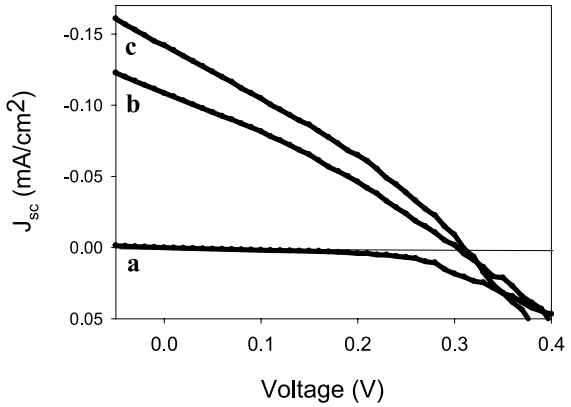

Fig. 4 I–V-curves performed to an HSC of the type ITO/SnO_2/MEH-PPV/Ag under ambient atmosphere: (**a**) dark, (**b**) with a UV filter (<400 nm), and (**c**) without a UV filter. Samples were stabilized in the dark under ambient atmosphere conditions before analyses. HSCs measured in ambient atmosphere with AM1.5 spectral distribution and 1000 W/m^2. Active area is 3.1 ± 0.2 cm^2. Polymer thickness is 110 nm

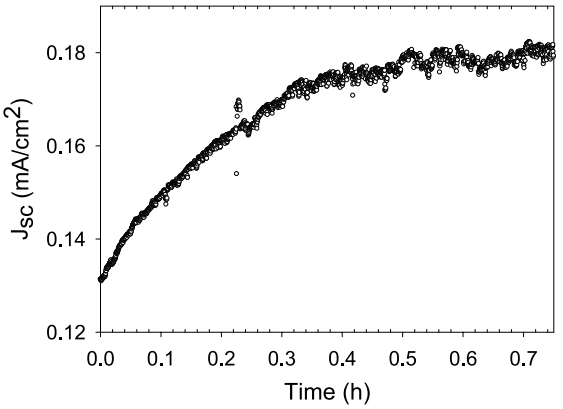

Fig. 5 An increase in J_{sc} observed during the first hour of solar decay analyses carried out to an HSC of the type ITO/$SnO_{2\ \text{thin film}}$/MEH-PPV/Ag. HSCs measured in ambient atmosphere with AM1.5 spectral distribution and 1000 W/m^2. Active area is 3.2 ± 0.1 cm^2. Polymer thickness is 110 nm

changes were observed on the I–V-curves as observed in Figs. 4(b) and 4(c). Almost the same voltage, about −0.32 V, and current densities between 0.14 mA/cm^2 and 0.17 mA/cm^2 were observed when the samples were analyzed with and without filter, respectively. The latter could indicate that the application of SnO_2 could be a good choice as electron transport material which neglects or decreases the degradation of the MEH-PPV polymer during irradiation under ambient atmospheres. In order to prove the latter, we carried out analyses of the HSC under long-term irradiation as described in the following section.

3.4 Stability under long-term irradiation

Stability analyses under constant irradiation conditions (1000 mW/cm^2) were performed to HSC of the type ITO/$SnO_{2\ \text{thin film}}$/MEH-PPV/Ag after the solar cell was stabilized in the dark. As shown in Fig. 5, we observed an initial increase in current density from 0.13 mA/cm^2 to about 0.18 mA/cm^2 in less than 1 hour. This improvement is characteristic of HSC applying thin film semiconductor oxides and has been linked to the re-adsorption of oxygen from the atmosphere into the semiconductor oxide during irradiation [8–12]. After reaching a maximum, J_{sc} stabilized and decreased steadily with time. This behavior is observed in all semiconductor oxides, and, in the case of HSC applying SnO_2, it was observed that the degradation was worse (faster degradation) than with Nb_2O_5 or TiO_2, CeO_2 or CeO_2–TiO_2 as can be seen from our previous work [8]. Only ZnO has been observed to degrade the polymer faster than SnO_2.

3.5 Comparison of SnO_2 with TiO_2, Nb_2O_5 and ZnO thin films

Finally, we would like to compare the response of HSC applying different thin film semiconductor oxides as analyzed before in our laboratory, TiO_2, Nb_2O_5, ZnO, and CeO-base oxides [8–12], and the one presented in this work applying SnO_2. In general, we have observed that the voltage of the HSC is dependent on the type of semiconductor oxide applied. The highest V_{oc} and J_{sc} have been observed for HSC applying TiO_2 and Nb_2O_5 (about −0.7 V) followed by SnO_2 with −0.5 V, ZnO with V_{oc} of about −0.3 V, and on the positive side CeO_2 with a value of +0.12 V and CeO_2–TiO_2 with a value of +0.42 V as shown in Table 1.

Similarities between HSCs are observed also on all I–V-curves which are characterized by low fill factors (never higher than 44%). This could be an indication of high internal resistances and leakage currents present in these systems, usually observed in devices with high recombination problems. Current leakages could come from the inhomogeneity of the oxide thin film or due to their thickness that are not more than a couple of tenths of nanometers (between 15 and 30 nm thick). In all cases, the degradation of the polymer with time and the decrease of photovoltaic properties have been inevitable when the HSC had the configuration applied in this work. The time it takes to degrade the polymer depends on the semiconductor oxide applied as follows (from the oxide showing the fastest degradation to the slowest): ZnO > SnO_2 > Nb_2O_5 > TiO_2 > CeO_2 > CeO_2–TiO_2.

4 Conclusions

Our results show the possibility to apply SnO_2 thin films as electron acceptors in HSC. Current densities of about

Table 1 Performance of HSCs applying thin film semiconductor oxides and the MEH-PPV polymer as reported in this work and in [8–12]

Semiconductor oxide	Bandgap	Stabilization time (h)	J_{sc} (mA/cm^2)[c]	V_{oc} (V)[d]	FF (%)
TiO_2	3.0–3.2 [23, 24]	2	0.42 ± 0.02	-0.74 ± 0.06	0.30 ± 0.03
Nb_2O_5[a]	2.3–3.4 [25]	48	0.28 ± 0.11	-0.64 ± 0.12	0.40 ± 0.04
Nb_2O_5[b]	2.3–3.4 [25]	48	0.34 ± 0.05	-0.40 ± 0.02	0.36 ± 0.03
SnO_2	3.1–3.0 [23]	1	0.20 ± 0.06	-0.50 ± 0.01	0.33 ± 0.03
ZnO	3.2–3.3 [28, 29]	2	0.30 ± 0.02	-0.38 ± 0.04	0.35 ± 0.05
CeO_2	3.0–3.2 [30–32]	120	0.004 ± 0.05	$+0.12 \pm 0.06$	0.25 ± 0.04
CeO_2–TiO_2	3.2–3.6 [26, 27]	50	0.007 ± 0.03	$+0.42 \pm 0.07$	0.32 ± 0.05

[a] ITO substrates on aluminosilicate glass

[b] ITO substrates on sodalime glass

[c] At maximum J_{sc}

[d] V_{oc} at the beginning, before stabilization. Active area is 3.3 ± 0.2 cm^2

$\sim$0.17 mA/cm^2, V_{oc} of $\sim$0.45 V, and 33% fill factors were achieved. Our HSC showed that an improvement in V_{oc} and fill factors can be obtained after the device is subjected to a stabilization period in the dark under ambient atmospheres. We have compared our results with other HSC applying different semiconductor oxides: TiO_2, Nb_2O_5 and ZnO, and found similar trends in photovoltaic behavior. We have suggested that this type of HSCs requires modification of device configuration to reach better performance and polymer stability. Nevertheless, the application of thin film semiconductor oxides in related electronic applications, such as hybrid transistors or hybrid OLEDs, is possible.

Acknowledgements We thank Dr. Frederik C. Krebs for a permission to analyze our samples in his laboratory. Also thanks to the Agència de Gestió d'Ajuts Universitaris i de Reserca (AGAUR, Catalunya Goverment), to the Canon Foundation in Europe, to the projects OTT2007-0423, OTT2007-0422 and OTT2007-1014 from the Spanish Ministry of Science and Innovation (MSI) and CDTI, and to the Consoider NANOSELECT project CSD2007-00041.

References

1. F. So, J. Kido, P. Borrows, Mater. Res. Soc. Bull. **33**, 663 (2008)
2. R.A.J. Janssen, J.C. Hummelen, N.S. Sariciftci, Mater. Res. Soc. Bull. **30**, 33 (2005)
3. C.J. Brabec, J.A. Hauch, P. Schilinsky, C. Waldauf, Mater. Res. Soc. Bull. **30**, 50 (2005)
4. C.J. Brabec, J.R. Durrant, Mater. Res. Soc. Bull. **33**, 670 (2008)
5. F.C. Krebs, Sol. Energy Mater. Sol. Cells **92**(7), 685 (2008)
6. F.C. Krebs, Sol. Energy Mater. Sol. Cells **92**(7), 715 (2008)
7. F.C. Krebs, K. Norrman, Prog. Photovolt. Res. Appl. **15**(8), 697 (2007)
8. M. Lira-Cantu, F.C. Krebs, Sol. Energy Mater. Sol. Cells **90**, 2076 (2006)
9. M. Lira-Cantu, F.C. Krebs, in *Rec. Res. Dev. Appl. Phys.*, ed. by S.G. Pandalai (Transworld Res. Network, 2005). ISBN:81-7895-187-8
10. M. Lira-Cantu, K. Norrman, J.W. Andreasen, F.C. Krebs, Chem. Mater. **18**, 5684–5690 (2006)
11. M. Lira-Cantu, K. Norrman, J.W. Andreasen, N. Casan-Pastor, F.C. Krebs, Electrochem. Trans. **3**(22), 1 (2007)
12. M. Lira-Cantu, P. Gómez-Romero, in *Hybrid Nanocomposites for Nanotechnology: Electronic, Optical, Magnetic and Bio/Medical Applications*, ed. by L. Merhari (Springer, Berlin, 2008). ISBN: 978-0-387-72398-3
13. H.J. Bolink, E. Coronado, D. Repetto, M. Sessolo, E.M. Barea, J. Bisquert, G. Garcia-Belmonte, J. Prochazka, L. Kavan, Adv. Funct. Mater. **18**(1), 145 (2008)
14. K. Morii, T. Kawase, S. Inoue, Appl. Phys. Lett. **92**(21), 213304 (2008)
15. N.A. Anderson, E. Hao, X. Ai, G. Hastings, T. Lian, Physica E Low-Dimens. Syst. Nanostruct. **14**, 215–218 (2002)
16. N.A. Anderson, E. Hao, X. Ai, G. Hastings, T. Lian, Chem. Phys. Lett. 347304-310 (2001)
17. H. Miyaoka, G. Mizutani, H. Sano, M. Omote, K. Nakatsuji, F. Komori, Solid State Commun. **123**, 399–404 (2002)
18. L.L. Diaz-Flores, R. Ramirez-Bon, A. Mendoza-Galvan, E. Prokhorov, J. Gonzalez-Hernandez, J. Phys. Chem. Solids **64**, 1037–1042 (2003)
19. H. Neugebauer, C.J. Brabec, J.C. Hummelen, R.A.J. Janssen, N.S. Sariciftci, Synth. Met. **121**, 35 (2001)
20. H. Meixner, U. Lampe, Sens. Actuators B **33**, 198–202 (1996)
21. J.E. Kroeze, T.J. Savenije, Thin Solid Films **451–452**, 54–59 (2004)
22. G. Benko, P. Myllyperkio, J. Pan, A.P. Yartsev, V. Sundstrom, J. Am. Chem. Soc. **125**(5), 1118–1119 (2003)
23. K. Kalyanasundaram, M. Grätzel, Coord. Chem. Rev. **177**, 347–414 (1998)
24. S.J. Pearton, C.R. Abernathy, M.E. Overberg, G.T. Thaler, D.P. Norton, J. Appl. Phys. **93**, 1–13 (2003)
25. N. Özer, D.-G. Chen, C.M. Lampert, Thin Solid Films **277**, 162–168 (1996)
26. F.E. Ghodsi, F.Z. Tepehan, G.G. Tepehan, Sol. Energy Mater. Sol. Cells. **68**, 355–364 (2001)

27. F.E. Ghodsi, F.Z. Tepehan, G.G. Tepehan, Electrochim. Acta **44**, 3127–3136 (1999)
28. L. Znaidi, G.J.A.A. Soler Illia, S. Benyahia, C. Sanchez, A.V. Kanaev, Thin Solid Films **428**, 257–262 (2003)
29. M.H. Aslan, A.Y. Oral, E. Mensur, A. Gül, E. Basaran, Sol. Energy Mater. Sol. Cells. **82**, 543–552 (2004)
30. B.S. Richards, Prog. Photovolt. Res. Appl. **12**, 253–281 (2004)
31. N. Özer, Sol. Energy Mater. Sol. Cells **68**, 391–400 (2001)
32. A. Corma, P. Atienzar, H. Garcia, J.-Y. Chane-Ching, Nat. Mater. **3**, 394–397 (2004)